

## A Global QCD Study of Direct Photon Production\*

J. Huston,<sup>d</sup> E. Kovacs,<sup>b,†</sup> S. Kuhlmann,<sup>a</sup> H. L. Lai,<sup>d</sup> J. F. Owens,<sup>c</sup>  
W. K. Tung<sup>d</sup><sup>a</sup>Argonne National Laboratory, <sup>b</sup>Fermi National Accelerator Laboratory,<sup>c</sup>Florida State University, <sup>d</sup>Michigan State University,<sup>†</sup>Visitor**Abstract**

A global QCD analysis of the direct photon production process from both fixed target and collider experiments is presented. These data sets now completely cover the parton  $x$  range from 0.01 to 0.6, thereby providing a stringent test of perturbative QCD and parton distributions. Previous detailed studies of direct photons emphasized fixed target data. We find most data sets have a steeper  $p_t$  distribution than the QCD prediction. Neither global fits with new parton distributions nor improved photon fragmentation functions can resolve this problem since the deviation occurs at different  $x$  values for experiments at different energies. A more likely explanation is the need for additional broadening of the  $k_t$  of the initial state partons. The magnitude and the possible physical origin of this effect are investigated and discussed.

---

\* This work was supported in part by DOE, NSF, and TNRLC.

# 1 Introduction

Direct photon production in hadron collisions is an important process to study in perturbative Quantum Chromodynamics (QCD) due to the clean measurement of photons, in contrast to jet physics with the jet definition uncertainties. In addition, sensitivity to the initial state gluon in the important Compton scattering mechanism provides a valuable opportunity to directly measure the gluon content inside the proton. These features have been utilized in studies [1] of earlier direct photon experiments in the context of next-to-leading-order (NLO) ( $\alpha\alpha_s^2$ ) QCD calculations of Aurenche *et al.* [2], and in the global analyses of parton distributions.[3, 4, 5] The potential usefulness of the direct photon experiments demonstrated in these works has yet to be fully realized due to the limited range of the fixed target experiments as well as remaining theoretical uncertainties related to scale-dependence and fragmentation processes.

In hadron colliders, earlier data from the ISR and  $Spp\bar{p}S$  colliders have been recently augmented by high statistics data from the Fermilab TEVATRON. The  $x$ -range covered by these collider and fixed-target experiments now spans the entire interval ( $0.01 < x < 0.6$ ). The combined range and improved accuracy of these data, as well as recent theoretical developments, provide a good opportunity to make a global comparison between theory and experiment. We report here such a study. The next two sections examine existing work on fixed-target and collider data and treat them in a unified context. A pattern of deviation of the observed  $x_t$  distribution from existing QCD expectations is highlighted. This is followed by a new global analysis of all existing data. We show that it is difficult to account for the observed pattern by new sets of parton (mostly gluon) distributions because the deviations occur at different  $x$  values for different experiments. Various alternative origins of the observed pattern and possible related phenomena in other processes are discussed.

## 2 Fixed Target Results

Previous parton distribution analyses incorporating direct photon data have focused on fixed target experiments, particularly the WA70 experiment (pp collisions at  $\sqrt{s} = 23$  GeV [6]) from CERN. The ABFOW [1] analysis performed fits on DIS data from the BCDMS experiment and used WA70 data as constraints to determine the gluon distribution, then checked many other direct photon experiments with the resulting parton distributions. The WA70 experimental normalization was fixed at unity.<sup>1</sup> The MRS analyses [3, 4] used a similar procedure but included more DIS data and added Drell-Yan results as constraints. Both of these groups used the “optimized scale” scheme [7] in choosing the renormalization and factorization scales. Fig. 1 shows the comparison of WA70 data with the ABFOW fit in the form (Data - NLO QCD)/NLO QCD as a function of photon  $x_t$  ( $2p_t/\sqrt{s}$ ). The production is fairly central so that photon  $x_t$  is approximately the parton  $x$  value probed. One sees that the fit is satisfactory. To see the scale-dependence of the NLO theory, one can compare the results obtained from two choices of scale, for example optimized and  $p_t/2$ . The latter is normalized to the former (as are the data points) and shown in the plot as the dashed line.

---

<sup>1</sup>Since the Compton cross-section is proportional to  $\alpha_s(\mu, \Lambda) \cdot G(x, \mu)$ , the normalization factor directly affects the determination of  $\Lambda$  and  $G(x, \mu)$ .

The optimization procedure results in higher cross-sections since it yields scales smaller than  $p_t/2$  for this kinematic region.

In the CTEQ2 global analysis[5], in addition to WA70, data from the fixed target experiments UA6 ( $pp$  collisions at  $\sqrt{s} = 24$  GeV [8]) and E706 (pBe collisions<sup>2</sup> at  $\sqrt{s} = 30.7$  GeV [10]) were used. These data were treated on the same footing as the DIS and Drell-Yan data in an overall global fit. The uncertainties on experimental normalization and theoretical scale-dependence are both taken into account in the analysis procedure (see Sec.4 and Ref.[5] for details). In Fig. 2 data from these three experiments are compared to the CTEQ2M fit. In this figure the more recent data from UA6 ( $pp$  and  $\bar{p}p$  collisions [11]), which agree with their earlier data, are shown. The absolute normalizations of all data and theory are used in this figure. These fixed-target experiments cover similar  $x_t$  ranges (with E706 extending somewhat lower) and are roughly consistent with each other. We note that the E706 data show a deviation from NLO QCD on this comparison plot which was not evident in previous comparisons with WA70 data alone. This pattern is also seen with other current parton distribution sets such as MRSD0 [4].

### 3 Collider Results and Calculations

The first direct photon data from hadron colliders came from the ISR  $pp$  collider[12], followed by the  $Spp\bar{p}S$  collider [13]. These data were found to be in qualitative agreement with NLO theory in Ref.[1]. However, the 1989 data from the TEVATRON  $\bar{p}p$  collider experiment CDF [14], extended into a new  $x$  region (0.01), and showed a clear deviation (1.5 – 2 times higher) from the NLO QCD predictions below  $p_t \sim 20$  GeV. Improved parton distribution sets such as CTEQ1 [5] and MRSD0 [4], using newer small- $x$  deep inelastic scattering data, removed approximately one-half of this discrepancy, but the remaining difference persisted. This effect has recently been confirmed with much higher statistics data from CDF [15]. The obvious source of uncertainty due to choice of scale cannot be responsible for the discrepancy since it produces small normalization shifts with no change in shape [14]. In addition, the optimized scales scheme, favored in fixed-target fits, was shown to make the disagreement between data and NLO QCD worse [14]. Thus, much attention has been directed to the proper theoretical treatment of *isolated* photon cross-sections (which the collider experiments measure) and the related issue of the photon fragmentation function.[16, 17, 18, 19] This is relevant since the collider kinematic range is sensitive to the *bremsstrahlung* process, where a photon is radiated off an initial or final state quark.

Analytic NLO calculations mentioned earlier [2] include the *bremsstrahlung* process, and use a leading-order (LO) fragmentation function in the region where the photon is emitted collinear to the quark. The implementation of the isolation cut in these calculations involves some approximations, and the (minor) effects of soft gluons inside the isolation cone are ignored. Alternatively, a Monte Carlo (MC) program for calculating NLO direct photon production (Baer *et al.* [18]) has proved to be very useful, particularly for colliders, since it provides a natural way to implement isolation cuts and the soft gluon effects. The MC calculation yields fully-inclusive cross sections within a few % of the analytic method. For

---

<sup>2</sup>The nuclear target dependence has been studied by E706 and is consistent with  $A^{1.0}$  for direct photon production[9].

calculations reported below, we compute the ratio of isolated-photon to total-inclusive cross sections using the MC method. We then use this ratio to put the collider and fixed-target data sets on the same footing in order to make a global comparison of data and the analytic calculations, and to perform new global fits for parton distributions. For the global fits, this procedure is also necessary since only the analytic form of the inclusive cross-section is efficient enough for the required repetitive calculations.

The analytic and MC programs mentioned above both use a LO fragmentation function convoluted with the LO two-jet production diagrams. There is now an analytic calculation from Gluck *et al.* [19] which uses a NLO parameterization of the photon fragmentation function convoluted with LO two-jet production, and NLO jet production convoluted with the LO photon fragmentation function. In Fig. 3, we compare this calculation, as well as that of Baer *et al.* [18], to the new CDF data. The two curves are evaluated with the same parton distributions (CTEQ2M) and scales ( $\mu = p_t$ ). The Gluck *et al.* calculation is 13% higher than Baer *et al.* uniformly in  $p_t$ . Thus the observed shape of the CDF data does not agree with either calculation. We note that the calculation of Ref. [19] used GRV [20] parton distributions and a scale of  $\mu = p_t/2$  (except for the fragmentation scale where  $\mu = (\text{Cone-size}) * p_t = 0.7 * p_t$  was used). The scale change leads to a 10% normalization shift upward, while the different parton distributions provide a 5% shape change at photon  $p_t = 16$  GeV. With these parameters the total fragmentation contribution to the isolated cross section was estimated in Ref. [19] to be  $\approx 10\%$ , hence any modification of this contribution is unlikely to explain the  $\approx 30\%$  difference in shape between the CDF data and NLO QCD calculation. In addition, the strength of the CDF data is in their small (5%) systematic uncertainty on the measured shape versus  $p_t$ , hence this new calculation is still insufficient to explain the data completely.

## 4 Global Comparison of Data and NLO QCD

The fixed-target and collider experiments described above together cover the photon  $x_t$  range from 0.01 to 0.6. It is natural to examine all the data at once in the framework of NLO QCD and to utilize the combined power of this rich collection of data in a new global NLO QCD+parton distribution analysis. In Fig.4 we show the compilation of data sets from colliders and fixed target experiments compared to NLO theory (using CTEQ2M parton distributions and  $\mu = p_t/2$ ). We see for the first time the impressive full coverage of the entire  $0.01 < x < 0.6$  range. We also see, however, that most of the data sets display a steeper dependence on  $x_t$  than is predicted by NLO QCD (horizontal line). We note that since both theory and experiment have inherent normalization uncertainties, it is difficult to discern an “excess” of photons at low  $p_t$  from a “deficit” at high  $p_t$ . However, the difference in slope between most data sets and the theory is quite apparent, and does not depend strongly on the experiment’s  $x_t$  range.

All previous global analyses used only fixed-target direct photon data in the fit. One obvious study is to perform a new global analysis including all the photon data in order to see to what extent new parton distributions, especially the gluon distribution which is not well constrained so far, could reduce the observed discrepancy. In this study, the most recent direct photon data from CDF [15] and UA6 (both  $pp$  and  $\bar{p}p$ ) [11] are included

together with UA2, R806, E706, WA70 and the standard DIS and Drell-Yan data sets used in the CTEQ2 global analysis [5]. The systematic errors for each experiment were separated into a normalization error (typically 10-15%) and point-to-point systematic errors that were added in quadrature with the statistical errors. The normalization for each experiment was allowed to vary from unity, constrained by the appropriate experimental errors as part of the  $\chi^2$  minimization procedure. The theoretical scale uncertainty was taken into account by assigning a “theoretical error” calculated using the difference obtained with scale choices of  $p_t/2$  and  $2p_t$ . The scale  $\mu$  was then allowed to vary during the minimization process as an overall parameter with the associated error.

Comparison of results from such a representative fit to the data points is shown in Fig. 5. The experiments are shown with their absolute normalization; in the fit they are renormalized downward by  $\approx 20\%$ . Qualitatively, this looks similar to Fig. 4. However, the CDF data do come closer to the theory, while the fixed target data in particular move farther away. Clearly, the small statistical and systematic errors of the CDF experiment cause this data set to dominate the fit, hence increasing the gluon density  $G(x, Q)$  in its  $x$ -range. This increase is compensated by a decrease in the gluon density in the large- $x$  region due to the momentum sum rule constraint.<sup>3</sup> This demonstrates, as expected, that it is difficult to improve the differing slopes by new parton distributions. Furthermore, we note that it is also difficult to attribute these differing slopes to the photon fragmentation function since the ISR and fixed target data are insensitive to fragmentation.

## 5 Discussion of Global Analysis Results

What could cause an effect seen in most experiments at low  $p_t$  irrespective of their  $x$  range? One possibility is that of “ $k_t$  smearing”, since any uniform smearing on a steeply falling  $p_t$  distribution enhances the low  $p_t$  end of the spectrum more than the high  $p_t$  end. The question is therefore: whether the NLO QCD calculation (involving at most one non-collinear initial state gluon) embodies sufficient  $k_t$  broadening of the initial state partons, or whether additional effects due to initial state multi-gluon radiation and non-perturbative physics (i.e. “intrinsic  $k_t$ ”) also need to be included?

In order to explore this problem in a simplistic fashion, the NLO QCD prediction for the cross section was convoluted with gaussian functions of transverse momentum. The effect of such a convolution is to induce corrections to the cross section that behave as  $\sim \sigma^2/p_t^2$ , where  $p_t$  is the photon  $p_t$  and  $\sigma$  is the width of the gaussian, representing the additional  $k_t$  in the system. The values of  $\sigma$  needed to reproduce approximately the collider data sets varied from  $\approx 2$ -3 GeV for R806, to  $\approx 3$ -4 GeV for UA2 and CDF. The corrections of course also depend on the local slope of the NLO QCD cross sections, therefore the fixed target experiments are extremely sensitive to  $\sigma$  due to their rapidly falling  $p_t$  spectra. A width of  $\approx 1$ -2 GeV for E706, and slightly smaller than 1 GeV for WA70 and UA6 gave a

---

<sup>3</sup>The momentum fraction carried by the gluon is constrained by the momentum sum rule to the range 0.42-0.43 in most current global parton analyses, since the total momentum fraction carried by quarks is very well determined by recent precision DIS experiments. We also note that the  $x$  range of the CDF data (0.01-0.1) carries a large percentage of the gluon momentum, given the general shape of the gluon distribution.

reasonable overall description of all the data sets. This exercise is, of course, completely ad hoc: it merely serves the purpose of indicating the approximate magnitudes of the smearing necessary to bridge the gap between the NLO QCD calculation and experiment. The energy dependence of the required smearing width reveals that this possible effect is probably not of a simple “intrinsic” type associated with the confinement size of the hadron, but more likely due to multiple gluon emissions.<sup>4</sup>

Smearing due to multiple gluon emissions is incorporated in many QCD shower MC programs. As another exercise, the QCD MC program PYTHIA [21] was utilized to generate the direct photon cross section for the CDF experiment used in our analysis. Within PYTHIA, there is the option to turn on/off initial state gluon radiation. We found that the ratios of cross sections (initial state radiation on/ initial state radiation off) show the same general pattern for the CDF data as seen in Figures 4 and 5. The MC program uses only LO hard matrix elements, and the relation of  $k_t$  smearing from the multiple gluons in this calculation to the fixed order NLO cross-section is not clear. However, it is obvious that physical effects due to multiple radiation have the general characteristics of the observed cross-section.

Theoretically, multiple gluon emission is the main physics effect treated systematically in the “ $p_t$  resummation” formalism of vector-boson production (continuum Drell-Yan, W, and Z production) [22]. Although, in principle,  $p_t$  resummation is not needed for inclusive direct photon production (because it is not strictly speaking a “multiple large scale” problem), it is intriguing to note that the resummed cross-section formula of Collins *et al.* [22] requires a “non-perturbative” broadening factor which bridges the  $p_t$  physics at the confinement and perturbative scales, and this broadening is inherently energy dependent. It is well worth exploring, both theoretically and phenomenologically, any possible relations between this result and the question at hand.

From an experimental point of view, one can investigate  $k_t$  effects directly by examining the  $p_t$  imbalance of diphoton states. WA70 [23] compared the distribution of diphoton system  $p_t$  with that predicted by NLO QCD smeared with a gaussian  $k_t$  broadening. They found that the typical width of 0.34 GeV intrinsic parton transverse momentum was insufficient to explain their data, while an additional broadening of 0.91 GeV gave a much improved fit. This extra broadening for diphotons is close to the amount that gave a reasonable overall description of the fixed target single photon measurements mentioned earlier. A similar situation exists for CDF diphotons [24]. Fig. 6 shows the diphoton system  $p_t$  from the data, NLO QCD and PYTHIA. The small statistics of the data do not provide strong discrimination at this time, but the important point is that the distribution from PYTHIA is significantly broader than NLO QCD. Once again if the NLO QCD prediction is smeared with a gaussian, a width of  $\approx 3$  GeV is needed to reproduce PYTHIA, and this is close to what was needed to bring the CDF *single* photons in agreement with NLO QCD. The

---

<sup>4</sup>In the previous analysis in ref. [1] mentioned earlier, there was no conclusion of the need for an additional contribution from initial state  $k_t$ . However, some elements were present in that analysis that might have masked this effect: (i) they emphasized the WA70 data, which are qualitatively consistent with NLO QCD without additional smearing; (ii) the low  $p_t$  data points from the ISR (where the deviation is most apparent) were removed in the analysis because the scale optimization failed; and (iii) the discrepancy between the low  $p_t$  data points of UA1 & UA2 and theory was attributed to uncertainties of photon fragmentation contribution and isolation cuts at the time (recent progress reviewed in Sec.3 has considerably reduced these uncertainties).

agreement in the magnitude of the broadening necessary for the diphotons and the single photons may be fortuitous, since the production processes are different. But the important point is that the diphotons indicate a potential problem with  $k_t$ , complementing the inclusive photon trends.

## 6 Conclusions and Future Prospects

In conclusion we have performed a global study of direct photon experiments spanning a wide range of parton  $x$  values. We see a pattern of deviation between the measured slopes versus photon  $p_t$  and the corresponding NLO QCD calculations. The deviations occur in several different experiments in different parton  $x$  ranges with widely varying sensitivities to photon fragmentation functions and theory scales. Thus it is difficult to invoke new parton distribution functions or a different treatment of the fragmentation process to explain all the data. This is verified by a new global parton distribution fit using all the direct photon data described in this paper. One possibility is the NLO QCD theory needs to be supplemented by additional  $k_t$  broadening from non-perturbative physics and/or initial state gluon radiation. A similar phenomenon has been seen in studies of the relative  $p_t$  of diphoton final states and this premise has been considered for some time [25]. We note that the same effect should also appear in low  $p_t$  measurements of other processes such as dijet and heavy flavor production. Low  $p_t$  dijet production typically has substantial systematic uncertainties [26], but the effects of  $k_t$  *have* been extensively studied in fixed target heavy flavor production [27], also with the conclusion for the need for additional  $k_t$  broadening. On the theoretical front, refinement of the treatment of  $k_t$  physics could take many different forms, from the analog of “non-perturbative functions” in Drell-Yan  $p_t$  resummation formalism (cf. previous section) and the  $k_t$ -dependent parton distributions associated with the new “high-energy factorization theorem” [28], to the interface of the parton shower calculations and NLO QCD (as performed for W production in [29]).

We clearly need a better understanding of the underlying physics before low- $p_t$  photon measurements can be confidently relied upon as the primary source of information on gluons in a global QCD analysis. For the time being, the better determination of the elusive  $G(x, Q)$  must depend on a variety of sources of information including DIS, direct photon, and differential jet cross-sections.

## 7 Acknowledgements

We thank Werner Vogelsang and Geoff Bodwin for useful discussions. This work was supported in part by the Department of Energy, National Science Foundation, and the Texas National Research Laboratory Commission.

# References

- [1] P. Aurenche et al. Phys. Rev. **D39**, 3275 (1989).
- [2] P. Aurenche et al. Nucl. Phys. **B286**, 553 (1987).
- [3] A. D. Martin, R. G. Roberts, W. J. Stirling. Phys. Rev. **D43**, 3648 (1991).
- [4] A. D. Martin, R. G. Roberts, W. J. Stirling. Phys. Lett. **B306**, 145 (1993).
- [5] CTEQ Collaboration: H.L. Lai et al. Preprint MSU-HEP-41024, CTEQ-404 (to be published).
- [6] M. Bonesini et al. (WA70 Collaboration). Z. Phys. **C38**, 371 (1988).
- [7] M. Fontannaz, P. Aurenche, R. Baier, and D. Schiff. Nucl. Phys. **B286**, 509 (1987).
- [8] A. Bernasconi et al. (UA6 Collaboration). Phys. Lett. **B206**, 163 (1988).
- [9] M. Zieliński et al. (E706 Collaboration). *Nuclear effects in high  $p_t$  production of neutral mesons and direct photons*, 5<sup>th</sup> Conference on the Interactions of Particle and Nuclear Physics, May, 1994
- [10] G. Alverson et al. (E706 Collaboration). Phys. Rev. **D48**, 5 (1993).
- [11] G. Sozzi et al. (UA6 Collaboration). Phys. Lett. **B317**, 243 (1993).
- [12] E. Anassontzis et al. (R806 Collaboration). Z. Phys. **C13**, 277 (1982) is used in this paper. There are numerous other ISR photon measurements, R806 has the widest  $p_t$  range and smallest uncertainties.
- [13] J. Alitti et al. (UA2 Collaboration). Phys. Lett. **B263**, 544 (1991) is used in this paper due to its smaller uncertainties compared to UA1. The two data sets are in complete agreement in slope and normalization.
- [14] F. Abe et al. (CDF Collaboration). Phys. Rev., **D48**, 2998 (1993).  
F. Abe et al. (CDF Collaboration). Phys. Rev. Lett., **68**, 2734 (1992).
- [15] F. Abe et al. (CDF Collaboration). Phys. Rev. Lett. **73**, 2662 (1994).
- [16] Edmond L. Berger and Jianwei Qiu, Phys. Rev. **D44**, 2002 (1991).
- [17] P. Aurenche et al. Nucl. Phys. **B399**, 34 (1993).
- [18] H. Baer, J. Ohnemus, and J.F. Owens. Phys. Rev. **D42**, 61 (1990).
- [19] M. Gluck et al. Phys. Rev. Lett. **73**, 388 (1994).

The calculations mentioned in the text that were not contained in this publication came from W. Vogelsang, private communication.



- [20] M. Gluck, E. Reya, A. Vogt. Phys. Lett. **B306**, 391 (1993).
- [21] PYTHIA 5.4 described in H. Bengtsson and T. Sjostrand, Comput. Phys. Commun. **46**, 43 (1987), was used to generate the diphoton events.
- [22] Y.L. Dokshitser et al., Phys. Rep. **B58**, 271 (1980); G. Altarelli et al., Nucl. Phys., **B246**, 12 (1984); J.C. Collins, D.E. Soper, and G. Sterman. Nucl. Phys. **B250**, 199 (1985)
- [23] E. Bonvin et al. (WA70 Collaboration). Phys. Lett. **B236**, 523 (1990).
- [24] F. Abe et al. (CDF Collaboration). Phys. Rev. Lett. **70**, 2232 (1993).
- [25] See for example the contributions from C. Bromberg and R. M. Harris to the *Proceedings of the Workshop on Hadron Structure Functions and Parton Distributions*, April 1990.
- [26] Eve Kovacs for the CDF Collaboration. *Testing QCD with Jet Physics at CDF*, July, 1994. FNAL-CONF-94/215-E.
- [27] S. Frixione et al. *Charm and Bottom Production: Theoretical Results Versus Experimental Data*, June, 1994. CERN-TH.7292/94
- [28] S. Catani et al., Phys. Lett. **B242**, 97 (1990) and Nucl. Phys. **B366**, 135 (1991); J.C. Collins and R.K. Ellis, Nucl. Phys. **B360**, 3 (1991); E.M. Levin et al., Sov. J. Nucl. Phys. 53, 657 (1991).
- [29] H. Baer and M. Reno. Phys. Rev. **D44**, 3375 (1991).

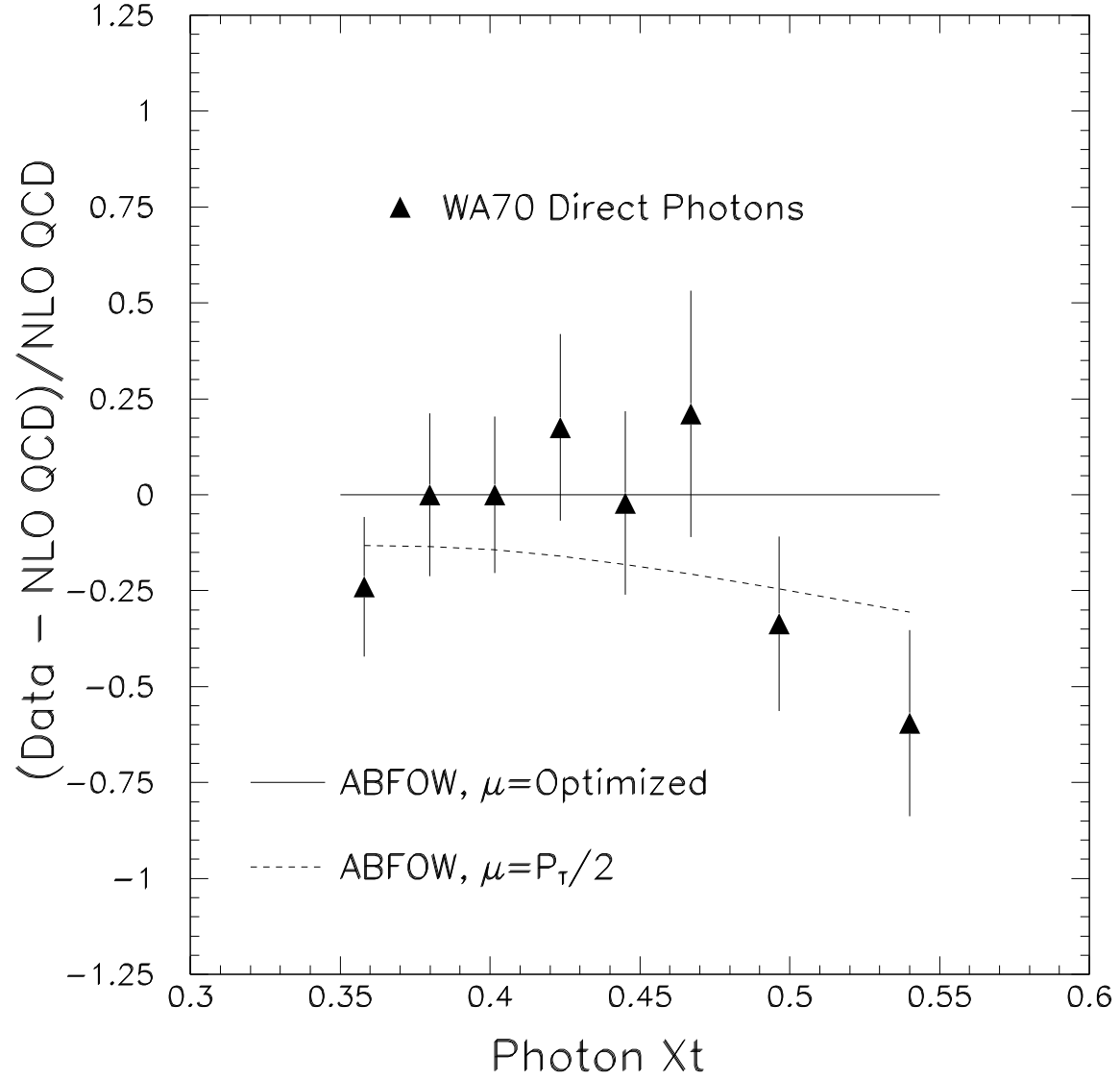


Figure 1: Direct photon production data from WA70 is compared to the NLO QCD fit of ABFOW using optimized scales. The fractional difference is shown in order to display details of the comparison. (see text)

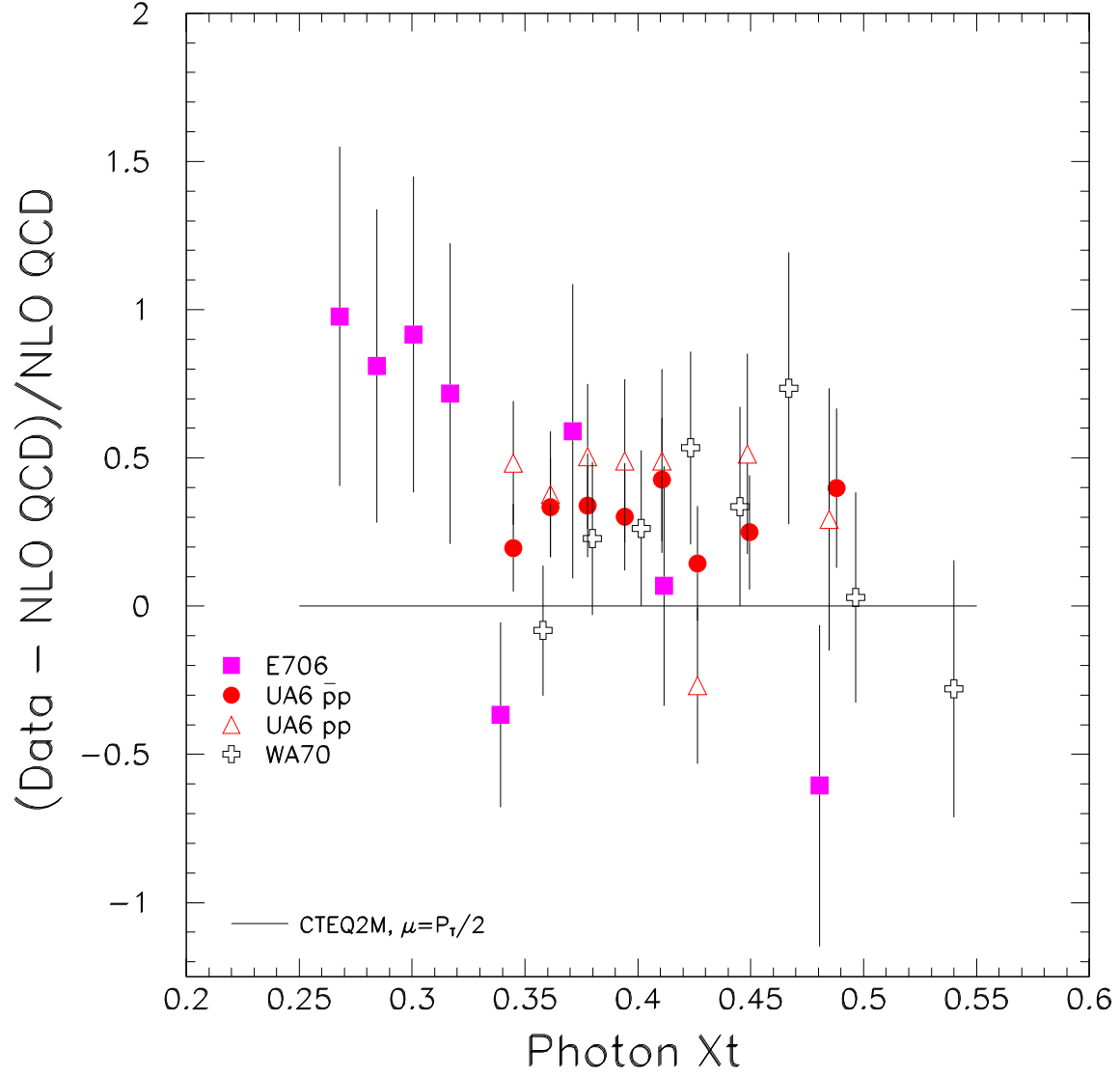


Figure 2: Fixed target direct photon experiments WA70, UA6, and E706 are compared to a NLO QCD results. Fractional differences between data points and the CTEQ2M fit are shown. (see text)

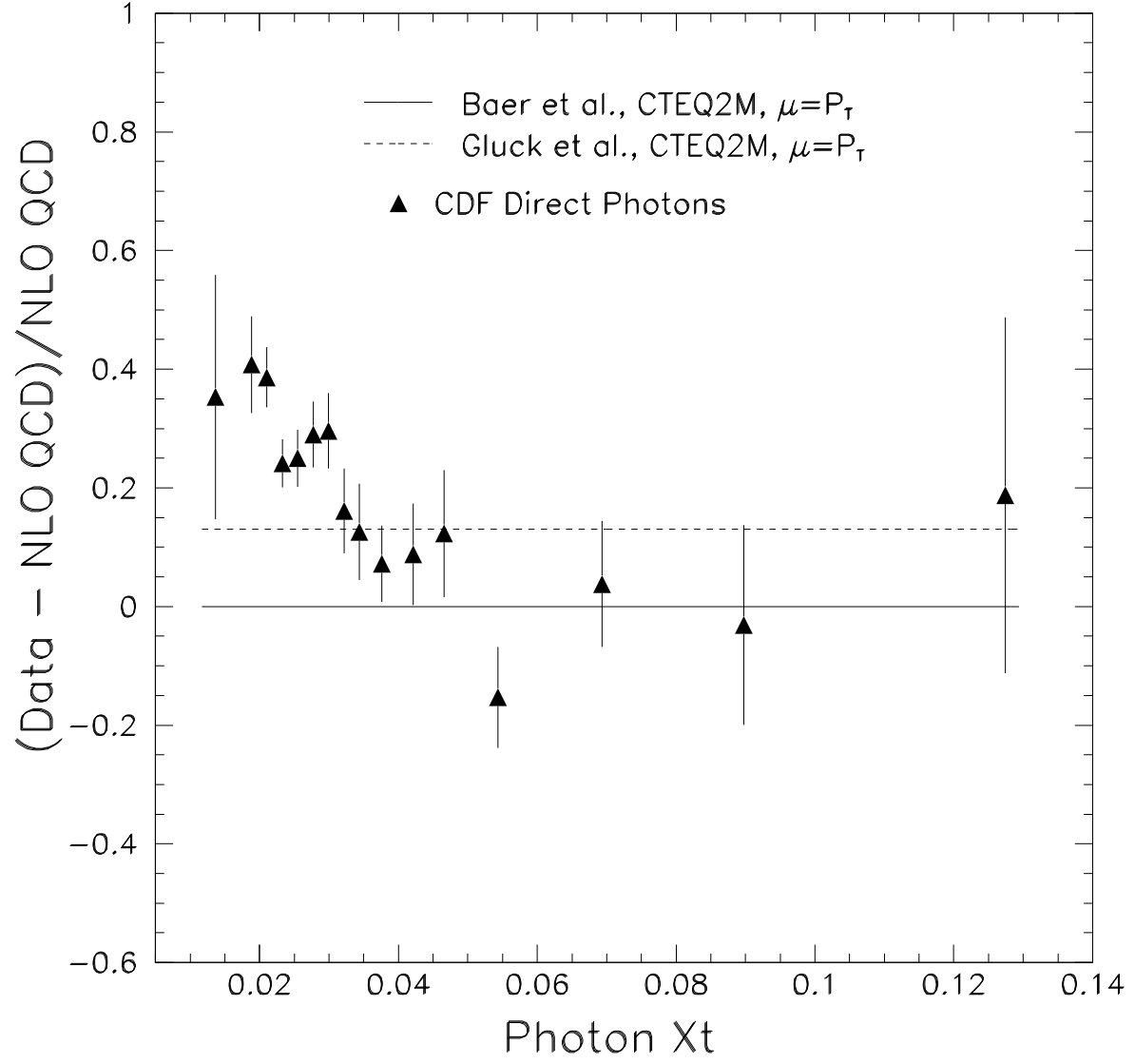


Figure 3: Direct photon data from the CDF experiment is compared to NLO QCD predictions. (see text)

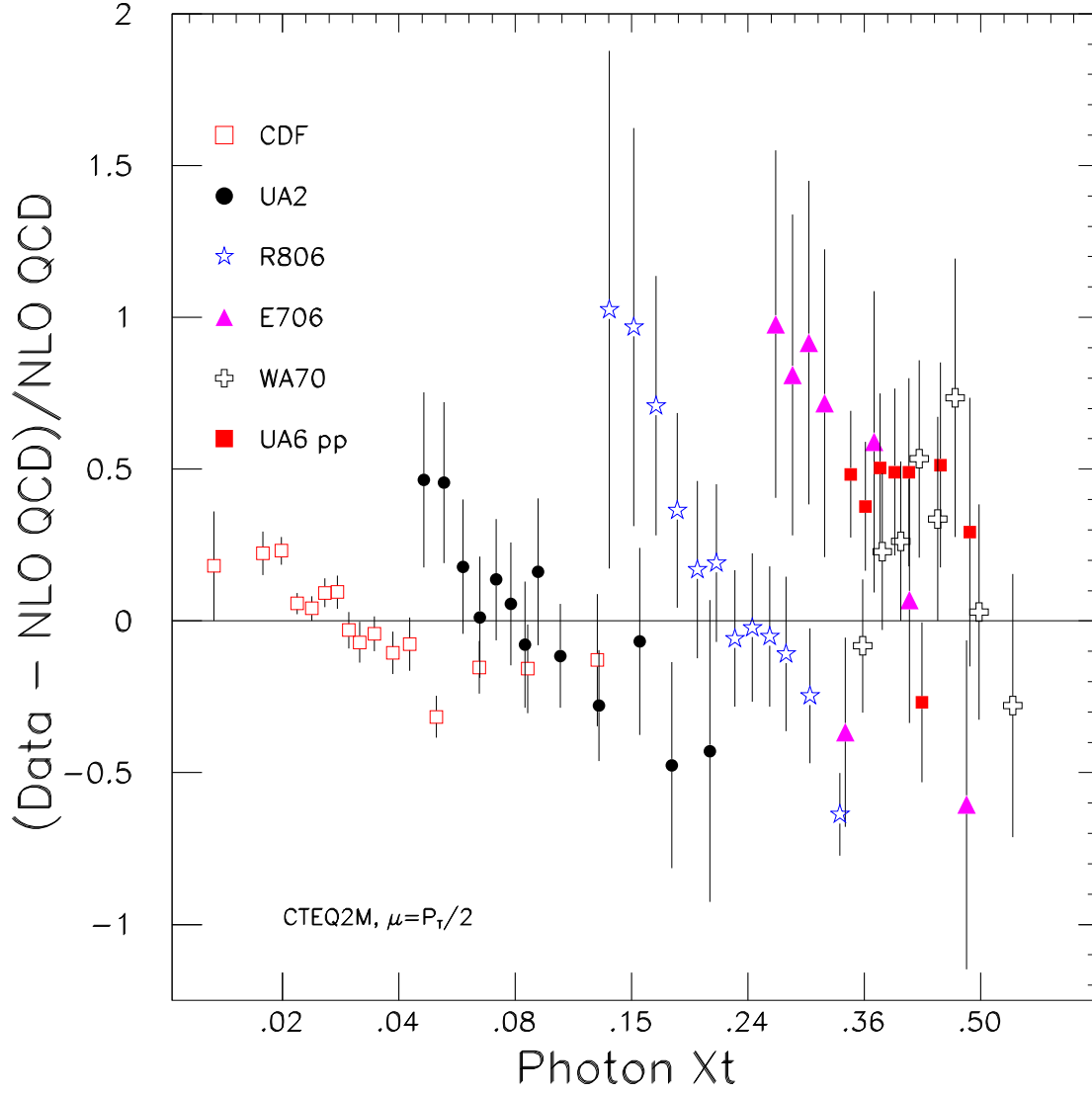


Figure 4: Compilation of direct photon experiments compared to NLO QCD predictions using CTEQ2M parton distributions. (see text)

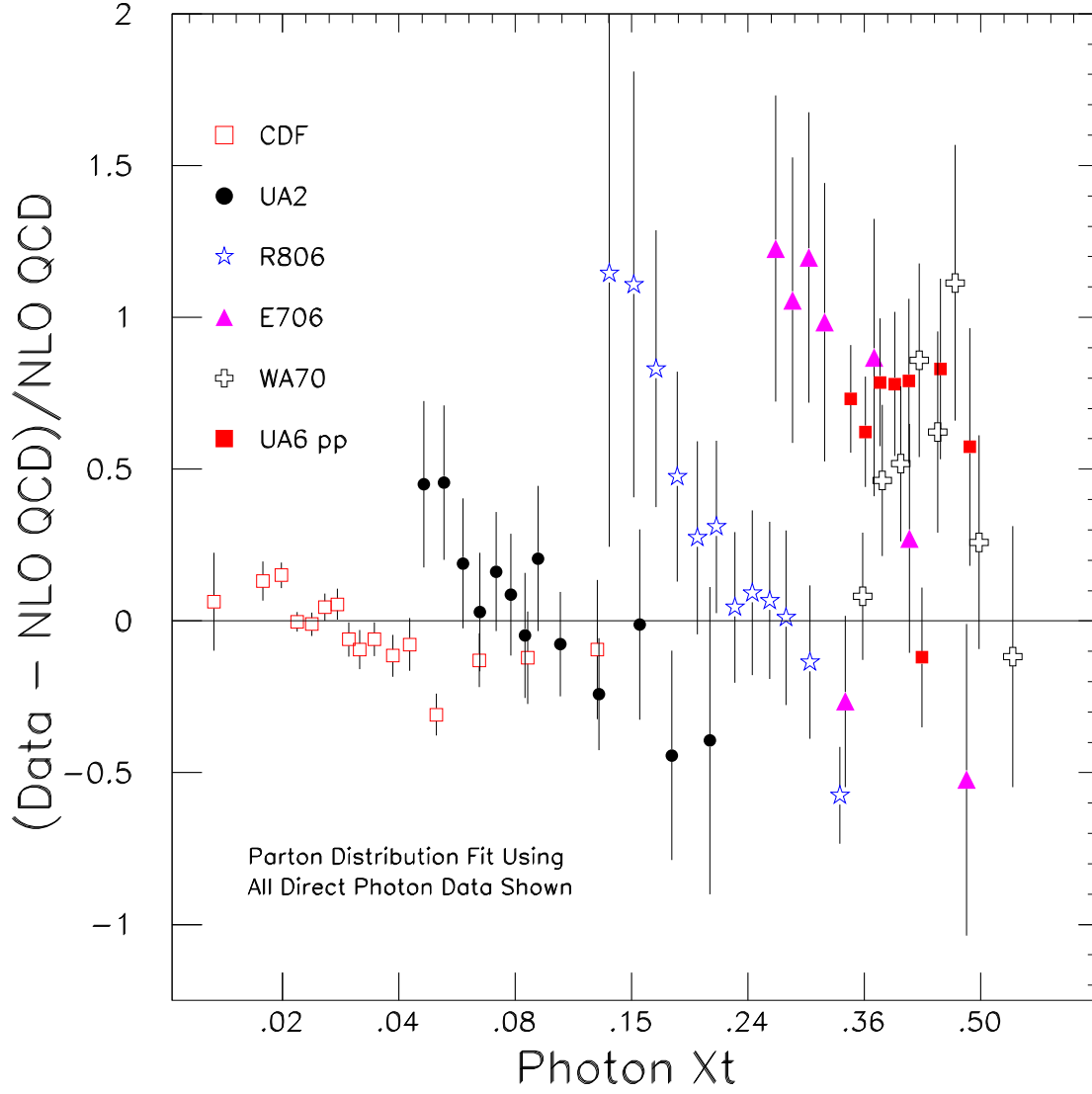


Figure 5: Compilation of direct photon experiments compared to a NLO QCD prediction using parton distributions fit using all the data shown. (see text)

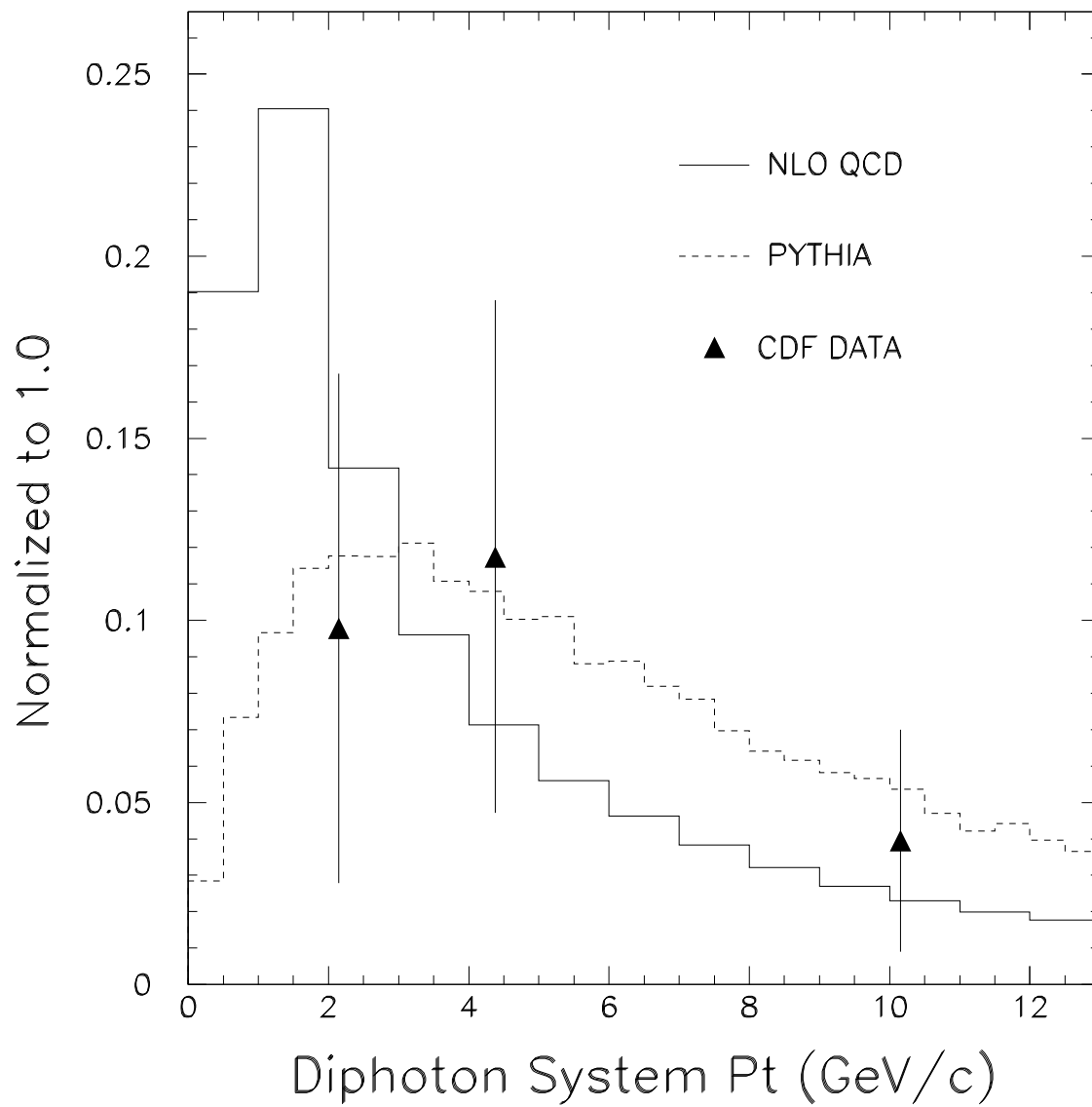


Figure 6: Diphoton system  $p_t$  distribution for PYTHIA, NLO QCD, and CDF data. (see text)